

## Formation of a Hybridization Gap in a Cage-like Compound $\text{CeFe}_2\text{Al}_{10}$

Yuji MURO<sup>1\*</sup>, Kiyochiro MOTOYA<sup>1</sup>, Yuta SAIGA<sup>2</sup>, and Toshiro TAKABATAKE<sup>2,3</sup>

<sup>1</sup>*Department of Physics, Faculty of Science and Technology, Tokyo University of Science, Noda  
278-8510*

<sup>2</sup>*Institute for Advanced Materials Research, Hiroshima University, Higashi-Hiroshima 739-8530*

<sup>3</sup>*Department of Quantum Matter, AdSM, Hiroshima University, Higashi-Hiroshima 739-8530*

We report on the magnetic, transport, and thermal properties of a cage-like compound  $\text{CeFe}_2\text{Al}_{10}$  that crystallizes in the orthorhombic  $\text{YbFe}_2\text{Al}_{10}$ -type structure. A broad peak in the magnetic susceptibility at 70 K indicates that  $\text{CeFe}_2\text{Al}_{10}$  is a valence fluctuation compound. The electrical resistivity and the Hall coefficient exhibit sharp upturns below 20 K, where the thermopower shows a rapid decrease. These low-temperature anomalies in the transport properties resemble those of a typical Kondo semiconductor  $\text{CeRhSb}$ . These features indicate the formation of a hybridization gap in  $\text{CeFe}_2\text{Al}_{10}$  on cooling below 20 K. The energy gap is estimated as 15 K from the thermal activation energy of the resistivity. The magnetic contribution of the specific heat shows a Schottky-type maximum at 30 K that provides another evidence for the gap formation in  $\text{CeFe}_2\text{Al}_{10}$ .

KEYWORDS:  $\text{CeFe}_2\text{Al}_{10}$ , cage-like structure, valence fluctuation, hybridization gap

---

\*Present address: Department of Quantum Matter, AdSM, Hiroshima University, Higashi-Hiroshima 739-8530

Among Ce-, Sm-, Yb-, and U-based intermetallics, there are a small number of compounds forming a narrow energy gap at the Fermi level. These materials are called as "hybridization gap semiconductors" or "Kondo semiconductors" because the energy gap originates from the strong hybridization between the localized 4f and conduction electrons, i.e. the *c-f* hybridization.<sup>1,2</sup> Most of the Ce-based hybridization-gap systems have been discovered within valence fluctuation compounds adopting certain crystal structures: the  $Y_3Sb_4Pt_3$ -type structure ( $Ce_3Bi_4Pt_3$  and  $Ce_3Sb_4T_3$  where  $T=Pt$  and  $Au$ ),<sup>3,4</sup> filled skutterudite one ( $CeT_4P_{12}$  where  $T=Fe, Ru, \text{ and } Os$ ),<sup>5,6</sup> and  $\epsilon$ -TiNiSi type one ( $CeNiSn, CeRhSb, CeRhAs, \text{ and } CeIrSb$ ).<sup>7-10</sup> The former two systems have a cubic symmetry and the latter has an orthorhombic one. The value of the hybridization gap ranges from 10 K to 1500 K,<sup>1</sup> which is two or three orders of magnitudes smaller than that of conventional semiconductors Si and Ge. Especially,  $CeNiSn$  and  $CeRhSb$  display the semiconducting behavior only below 10 K. The single-crystal studies<sup>7,11</sup> indicated that the magnetic and transport properties of  $CeNiSn$  and  $CeRhSb$  are highly anisotropic owing to the crystal-field effect, which also gives rise to the anisotropic gap.<sup>12</sup>

$CeFe_2Al_{10}$  crystallizes in the orthorhombic  $YbFe_2Al_{10}$ -type structure.<sup>13</sup> The crystal structure is shown in Fig. 1. One of the structural features is that the atomic distance between the nearest Ce-Ce ( $>5 \text{ \AA}$ ) is larger than those between the Ce and ligand Fe/Al atoms. Moreover, the nearest Ce-Al distance is  $3.1 \text{ \AA}$  which is comparable with that of the Ce-P distance in the filled skutterudite  $CeFe_4P_{12}$ . Thus, the  $YbFe_2Al_{10}$ -type rare-earth intermetallics can be viewed as cage compounds in which the rare-earth atom is accommodated in the large 4Fe-16Al polyhedron.

In this letter, we present the results of the magnetic susceptibility, electrical resistivity, Hall coefficient, thermopower, and specific heat measurements on a polycrystalline  $\text{CeFe}_2\text{Al}_{10}$  and its La counterpart. Our results indicate that  $\text{CeFe}_2\text{Al}_{10}$  is a new valence fluctuation compound forming a narrow hybridization gap with the value  $\Delta/k_B \sim 15$  K below 20 K.

Polycrystalline samples of  $\text{CeFe}_2\text{Al}_{10}$  and  $\text{LaFe}_2\text{Al}_{10}$  were synthesized by arc-melting the stoichiometric amounts of constituent elements under a Ti-gettered Ar atmosphere. Obtained buttons were annealed in an evacuated quartz ampoule at 800 °C for one week. Powder x-ray diffraction patterns confirmed that the both compounds crystallize in the  $\text{YbFe}_2\text{Al}_{10}$ -type structure (space group  $Cmcm$ , No. 63). The least-square refinements indicated the lattice parameters as  $a = 8.992$  Å,  $b = 10.216$  Å, and  $c = 9.065$  Å for  $\text{CeFe}_2\text{Al}_{10}$  and  $a = 9.050$  Å,  $b = 10.250$  Å, and  $c = 9.121$  Å for  $\text{LaFe}_2\text{Al}_{10}$ . These parameters are consistent with those reported by Thiede *et al.*<sup>13</sup> The electron-probe micro-analysis (EPMA) indicates the composition  $\text{Ce:Fe:Al} \simeq 1.00:1.95:10.1$ . No impurity phases were detected by the x-ray diffraction nor EPMA.

The magnetic susceptibility  $M/B$  was measured by using a commercial SQUID magnetometer (Quantum Design MPMS) from 2 K to 400 K. Electrical resistivity  $\rho$  measurements were performed by an ac four-probe method. Hall coefficient  $R_H$  for  $\text{CeFe}_2\text{Al}_{10}$  under 2 T was measured by an ac five-probe technique. The data were taken for two opposite  $B$  directions and corrected by  $(R_H(B) - R_H(-B))/2$  in order to eliminate the effect of residual unbalance of the voltage contacts. The specific heat  $C$  was measured by using a relaxation method. Measurements of  $\rho(T)$ ,  $R_H(T)$ , and  $C(T)$  were carried out between 2 K and 300 K

by using a commercial Quantum Design PPMS cryostat with a 9 T superconducting magnet. Thermopower  $S(T)$  for  $\text{CeFe}_2\text{Al}_{10}$  was measured by a differential method from 5 K to 300 K with a temperature gradient 0.05–0.5 K.

Figure 2 shows the temperature dependence of  $M/B$  for  $\text{CeFe}_2\text{Al}_{10}$  and  $\text{LaFe}_2\text{Al}_{10}$ .  $\text{LaFe}_2\text{Al}_{10}$  exhibits a nearly temperature-independent paramagnetism, indicating that the Fe atoms carry no magnetic moment. On the other hand,  $M/B$  for  $\text{CeFe}_2\text{Al}_{10}$  obeys a Curie-Weiss law,  $M/B = C/(T - \theta_p)$ , from 400 K down to 100 K. A least-square fitting to the data above 100 K indicates the effective magnetic moment  $\mu_{eff} = 2.78\mu_B$  and the paramagnetic Curie temperature  $\theta_p = -440$  K. The value of  $\mu_{eff}$  is slightly larger than that expected for a  $\text{Ce}^{3+}$  free ion ( $2.54\mu_B$ ). This discrepancy should be caused from the effect of crystal-field anisotropy in  $M/B$  because a strong anisotropy for the physical properties of  $\text{CeFe}_2\text{Al}_{10}$  is expected from the asymmetric Fe-Al cage shown in Fig. 1. In addition, a large negative value of  $\theta_p$  suggests the strong  $c$ - $f$  hybridization. At low temperatures,  $M/B$  shows a broad maximum at  $T_{max}^{M/B} \sim 70$  K that is reminiscent of  $M/B$  for  $\text{Ce}_3\text{Bi}_4\text{Pt}_3$  ( $T_{max}^{M/B} \sim 80$  K).<sup>3</sup> These features indicate that  $\text{CeFe}_2\text{Al}_{10}$  is a valence fluctuation compound. The numerical calculation of the susceptibility using the Coqblin-Schrieffer model for  $J = 5/2$ <sup>14</sup> gives a maximum at  $T_{max}^{M/B} \simeq 0.25T_K/W$  where  $T_K$  is the characteristic Kondo temperature and  $W \simeq 4\pi \times 0.103$  is the Wilson's value.<sup>15</sup> From this relation, we obtained  $T_K \simeq 360$  K for  $\text{CeFe}_2\text{Al}_{10}$ .

Figure 3(a) displays the results of  $\rho(T)$  for  $\text{CeFe}_2\text{Al}_{10}$  and  $\text{LaFe}_2\text{Al}_{10}$ . With decreasing temperature,  $\rho(T)$  for  $\text{LaFe}_2\text{Al}_{10}$  exhibits a monotonic decrease that is typical for metals. No superconducting transitions were observed down to 1.8 K. On the other hand,  $\rho(T)$  for

CeFe<sub>2</sub>Al<sub>10</sub> displays a logarithmic increase with decreasing  $T$  down to 70 K at which a maximum appears. This Kondo-type temperature dependence in  $\rho$  confirms the existence of strong  $c$ - $f$  hybridization in CeFe<sub>2</sub>Al<sub>10</sub>. Below 20 K,  $\rho(T)$  raises rapidly with decreasing  $T$ . Semiconducting behavior is manifested by a linear variation in  $\ln \rho$  versus  $1/T$  plot as shown in the inset of Fig. 3(a). A least-square fit to the  $\rho$  data between 10 K and 20 K by using the activation-type relation,  $\rho(T) \propto \exp(\Delta/2k_B T)$ , yields the energy gap  $\Delta/k_B = 15$  K.

The gap formation below 20 K is also recognized by a sharp increase in  $R_H$  as depicted in Fig. 3(b). The value of  $\Delta$  calculated from the  $\ln R_H$  vs  $1/T$  plot (inset of Fig. 3(b)) is 18 K that agrees with the value obtained from  $\rho$ . A small anomaly at 40 K in  $R_H$  should be caused from an extrinsic effect on the measurement.

Figure 3(c) displays the temperature dependence of  $S$  for CeFe<sub>2</sub>Al<sub>10</sub>. At 130 K,  $S(T)$  exhibits a broad maximum due to the strong  $c$ - $f$  hybridization. Such a maximum in  $S(T)$  has been reported for typical valence-fluctuation compounds CePd<sub>3</sub> and CeSn<sub>3</sub>.<sup>16</sup> Below 20 K,  $S(T)$  drops rapidly and changes the sign to negative at 13 K whereas  $R_H$  remains positive. This feature is similar to that observed in the polycrystalline CeRhSb.<sup>17</sup> The sharp drop in  $S(T)$  at 20 K should originate from the development of the hybridization gap because the semiconducting behavior appears at the same temperatures in  $\rho$  and  $R_H$ . The observed variation of  $S(T)$  resembles that calculated for the Kondo semiconductor using the periodic Anderson model.<sup>18</sup>

Figure 4 shows the magnetic contribution of the specific heat  $C_m$  divided by temperature for CeFe<sub>2</sub>Al<sub>10</sub>. Thereby, the data of  $C(T)$  for LaFe<sub>2</sub>Al<sub>10</sub> were subtracted from that for

CeFe<sub>2</sub>Al<sub>10</sub>.  $C_m/T$  shows a Schottky-type peak at 30 K, which is typical for the hybridization-gap systems.<sup>2</sup> For CeNiSn and CeRhSb, the  $C_m/T$  peak was explained by a V-shaped gap in the Lorentzian density of states (DOS).<sup>19</sup> We tried to analyze the present data by this model and show the calculation by the dashed line in Fig. 4. The temperature and height of the peak are reproduced with the width of Lorentzian DOS  $D/k_B = 180$  K and the gap  $\Delta/k_B = 100$  K, but the observed peak is sharper than that of calculated one.

The inset of Fig. 4 is the low-temperature part of  $C/T$  versus  $T^2$  plot. A linear fit for LaFe<sub>2</sub>Al<sub>10</sub> indicates the Sommerfeld coefficient  $\gamma \simeq 18$  mJ/mol·K<sup>2</sup> and the Debye temperature  $\theta_D \simeq 540$  K. On the other hand, the estimated  $\gamma \simeq 14$  mJ/mol·K<sup>2</sup> for CeFe<sub>2</sub>Al<sub>10</sub> is smaller than that of LaFe<sub>2</sub>Al<sub>10</sub>. Such a reversal in  $C/T$ , i.e.,  $\gamma(\text{Ce compound}) < \gamma(\text{La compound})$ , is reported only on Ce<sub>3</sub>Bi<sub>4</sub>Pt<sub>3</sub> and La<sub>3</sub>Bi<sub>4</sub>Pt<sub>3</sub>.<sup>3</sup> Hundley *et al.* argued that the residual  $\gamma$  in Ce<sub>3</sub>Bi<sub>4</sub>Pt<sub>3</sub> should disappear for the ideal system because they observed sample dependencies for the  $\gamma$  value and the Curie tail in the susceptibility at low temperatures. Indeed, a small shoulder at 10 K may be due to the effect of an impurity band located within the hybridization gap.<sup>20</sup> The impurity band may originate from some sort of imperfections because no impurity phases were detected. The imperfection can be responsible for the upturn in  $M/B$  below 9 K as shown in Fig. 2.

In summary, we measured the magnetic susceptibility, electrical resistivity, Hall coefficient, thermopower, and specific heat of CeFe<sub>2</sub>Al<sub>10</sub> with a caged structure. A broad maximum at 70 K in the magnetic susceptibility and a Kondo-lattice behavior in the electrical resistivity indicate that CeFe<sub>2</sub>Al<sub>10</sub> is a valence-fluctuation compound. The formation of the hybridization

gap below 20 K is manifested by the activation-type temperature variations in the resistivity and Hall coefficient, a sharp drop in the thermopower, and a Schottky-type anomaly in the specific heat. The value of the hybridization gap is estimated as 18~20 K from the resistivity and Hall coefficient.

This work was supported by Grant-in-Aid for Scientific Research from MEXT of Japan, Grant Nos. 18204032, 19051011, and 20102004.

**References**

- 1) G. Aeppli and Z. Fisk: Comments Cond. Mat. Phys. **16** (1992) 155.
- 2) P. S. Riseborough: Adv. Phys. **49** (2000) 257.
- 3) M. F. Hundley, P. C. Canfield, J. D. Thompson, and Z. Fisk: Phys. Rev. B **42** (1990) 6842.
- 4) M. Kasaya, K. Katoh, and K. Takegahara: Solid State Commun. **78** (1991) 797.
- 5) G. Meisner, M. S. Torikachvili, K. N. Yang, M. B. Maple, and R. P. Guertin: J. Appl. Phys. **57** (1985) 3073.
- 6) I. Shirovani, T. Uchiumi, C. Sekine, M. Hiro, S. Kimura, and N. Hamaya: J. Solid State Chem. **142** (1999) 146.
- 7) T. Takabatake, F. Teshima, H. Fujii, S. Nishigori, T. Suzuki, T. Fujita, Y. Yamaguchi, J. Sakurai, and D. Jaccard: Phys. Rev. B **41** (1990) 9607.
- 8) S. K. Malik and D. T. Adroja: Phys. Rev. B **43** (1991) 6277.
- 9) S. Yoshii, M. Kasaya, H. Takahashi, and N. Mori: Physica B **223-224** (1999) 421.
- 10) Y. Kawasaki, M. Izumi, Y. Kishimoto, T. Ohno, H. Tou, Y. Inaoka, M. Sera, K. Shigetoh, and T. Takabatake: Phys. Rev. B **75** (2007) 094410.
- 11) T. Takabatake, H. Tanaka, Y. Bando, H. Fujii, S. Nishigori, T. Suzuki, T. Fujita, and G. Kido: Phys. Rev. B **50** (1994) 623.
- 12) H. Ikeda and K. Miyake: J. Phys. Soc. Jpn. **65** (1998) 1769.
- 13) V. M. T. Thiede, T. Ebel, and W. Jeitschko: J. Mater. Chem. **8** (1998) 125.
- 14) V. T. Rajan: Phys. Rev. Lett. **51** (1983) 308.
- 15) N. Andrei and J. H. Lowenstein: Phys. Rev. Lett. **46** (1981) 356.
- 16) D. Jaccard and J. Sierro: *Valence Instabilities*, ed. P. Wachter and H. Boppart (North-Holland, Amsterdam, 1982), p. 409.
- 17) T. Takabatake, G. Nakamoto, H. Tanaka, Y. Bando, H. Fujii, S. Nishigori, H. Goshima, T. Suzuki,

T. Fujita, I. Oguro, T. Hiraoka, and S. K. Malik: Physica B **199-200** (1994) 457.

18) T. Saso and K. Urasaki: J. Phys. Chem. Solids **63** (2002) 1475.

19) S. Nishigori, H. Goshima, T. Suzuki, T. Fujita, G. Nakamoto, H. Tanaka, T. Takabatake, and H.

Fujii: J. Phys. Soc. Jpn. **65** (1996) 2614.

20) R. Shiina: J. Phys. Soc. Jpn. **64** (1995) 702.

Fig. 1. Crystal structure of  $\text{CeFe}_2\text{Al}_{10}$  with the orthorhombic  $\text{YbFe}_2\text{Al}_{10}$ -type structure. The distorted Fe-Al polyhedron filled with Ce is displayed

Fig. 2. Temperature dependence of the magnetic susceptibility for  $\text{CeFe}_2\text{Al}_{10}$  (closed circles) and  $\text{LaFe}_2\text{Al}_{10}$  (solid line). The dotted line represents the fitting result of the Curie-Weiss law for  $T > 100$  K.

Fig. 3. Temperature variations of (a) electrical resistivity, (b) Hall coefficient, and (c) thermopower for  $\text{CeFe}_2\text{Al}_{10}$ . The resistivity of  $\text{LaFe}_2\text{Al}_{10}$  is also shown in (a). The insets of (a) and (b) represent the Arrhenius plots of the resistivity and Hall coefficient, respectively.

Fig. 4. Temperature dependence of the magnetic contribution of the specific heat divided by temperature for  $\text{CeFe}_2\text{Al}_{10}$ . The dashed line represents the  $C/T$  calculated using the V-shaped gap model with  $D/k_B = 180$  K and  $\Delta/k_B = 100$  K. The inset shows the  $C/T$  versus  $T^2$  plot for  $\text{CeFe}_2\text{Al}_{10}$  (closed circles) and  $\text{LaFe}_2\text{Al}_{10}$  (solid line) for  $T < 7$  K.

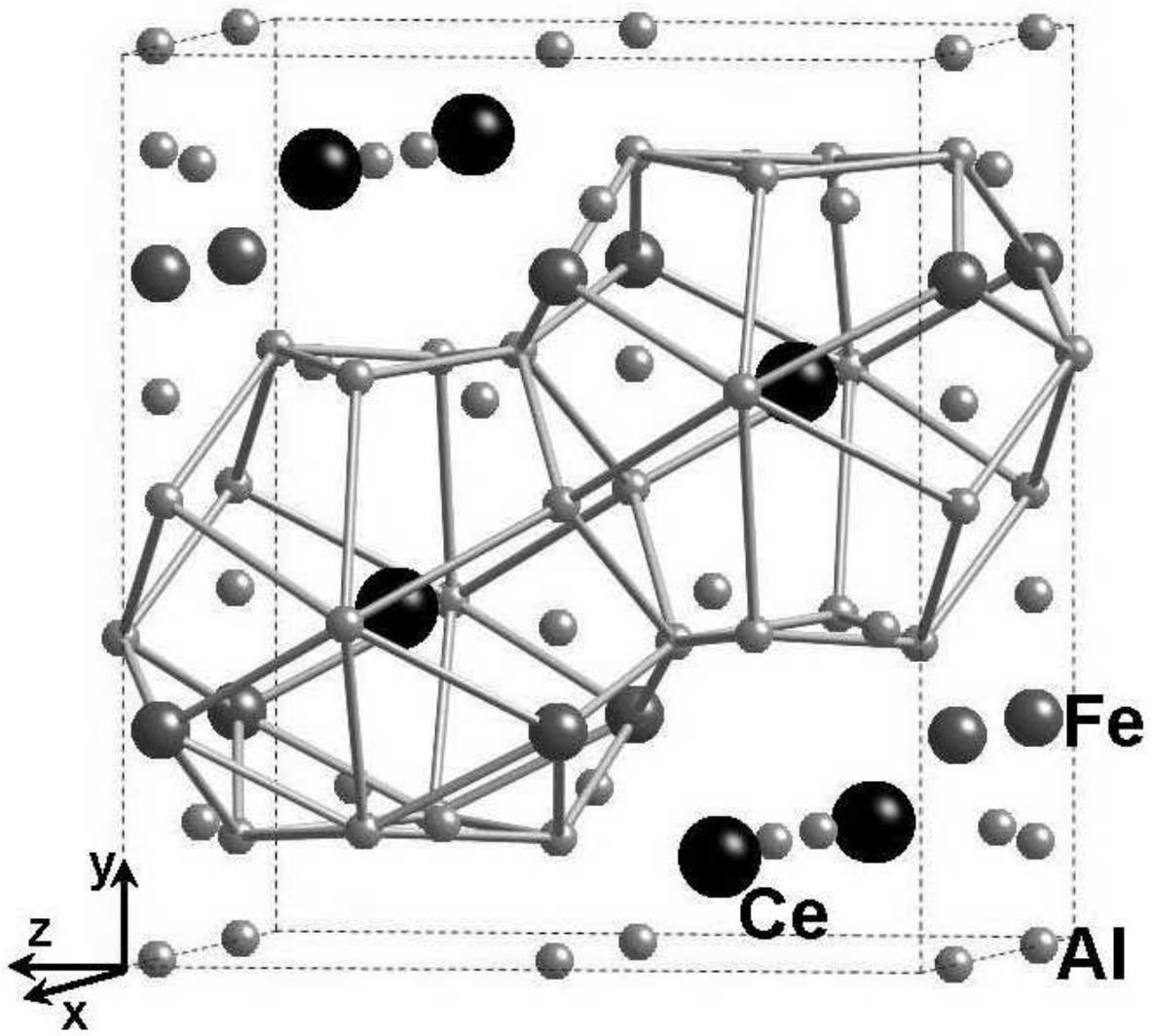


Fig. 1

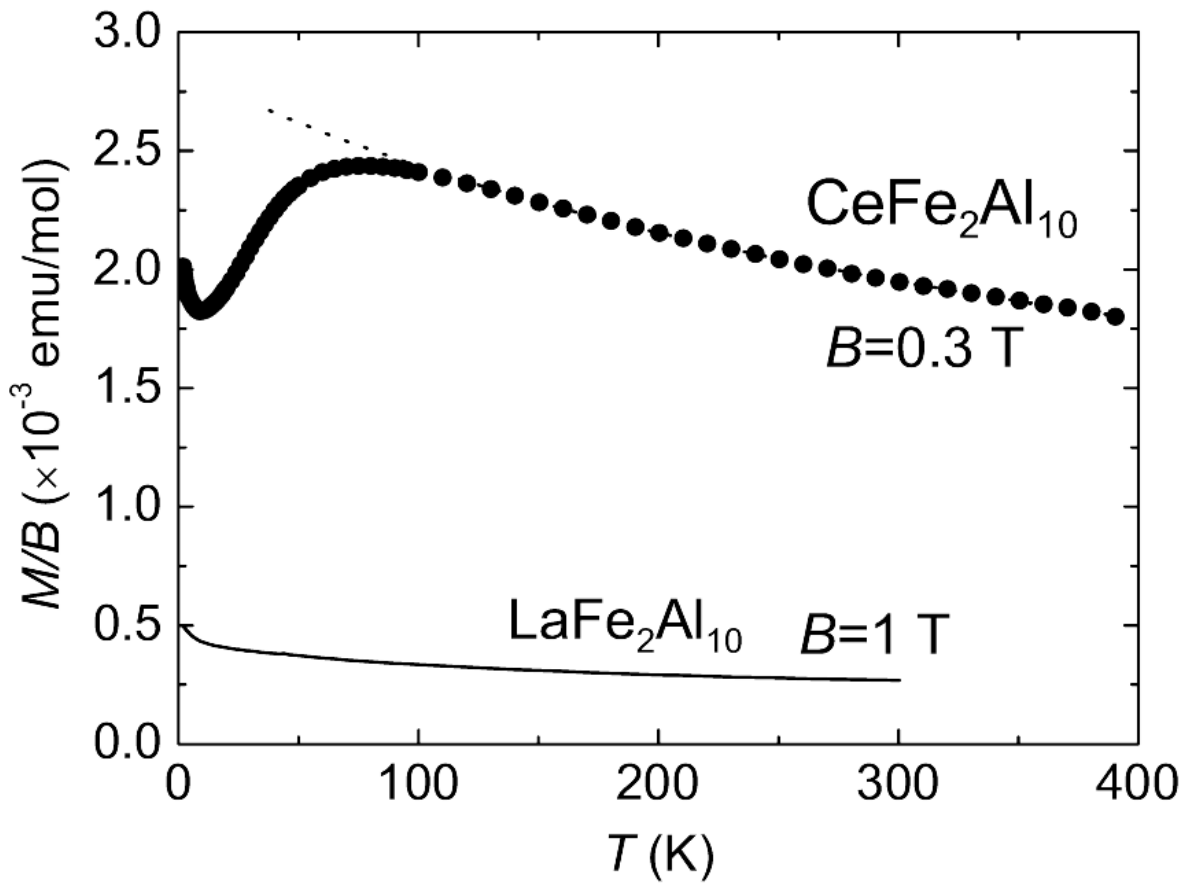


Fig. 2

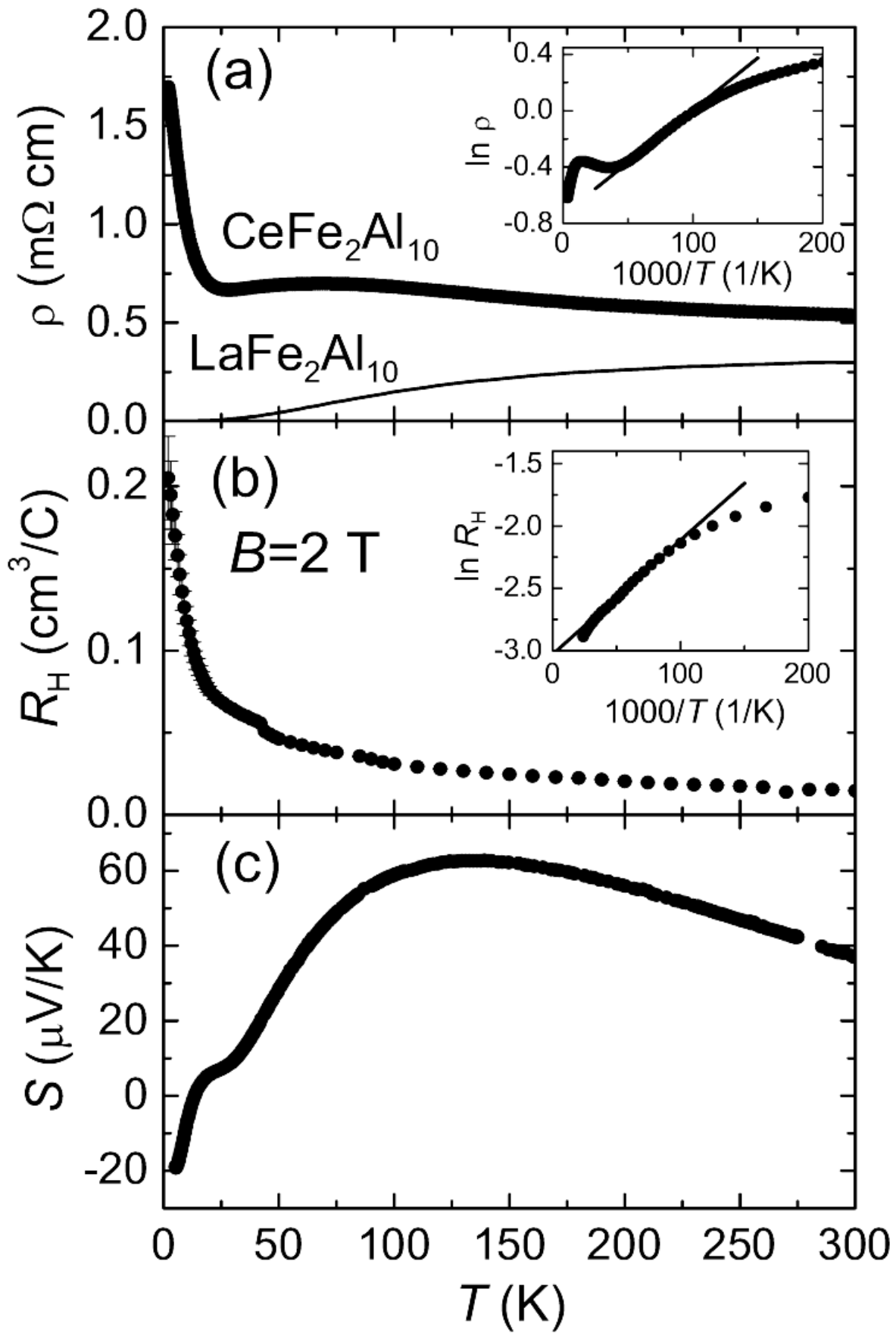


Fig. 3

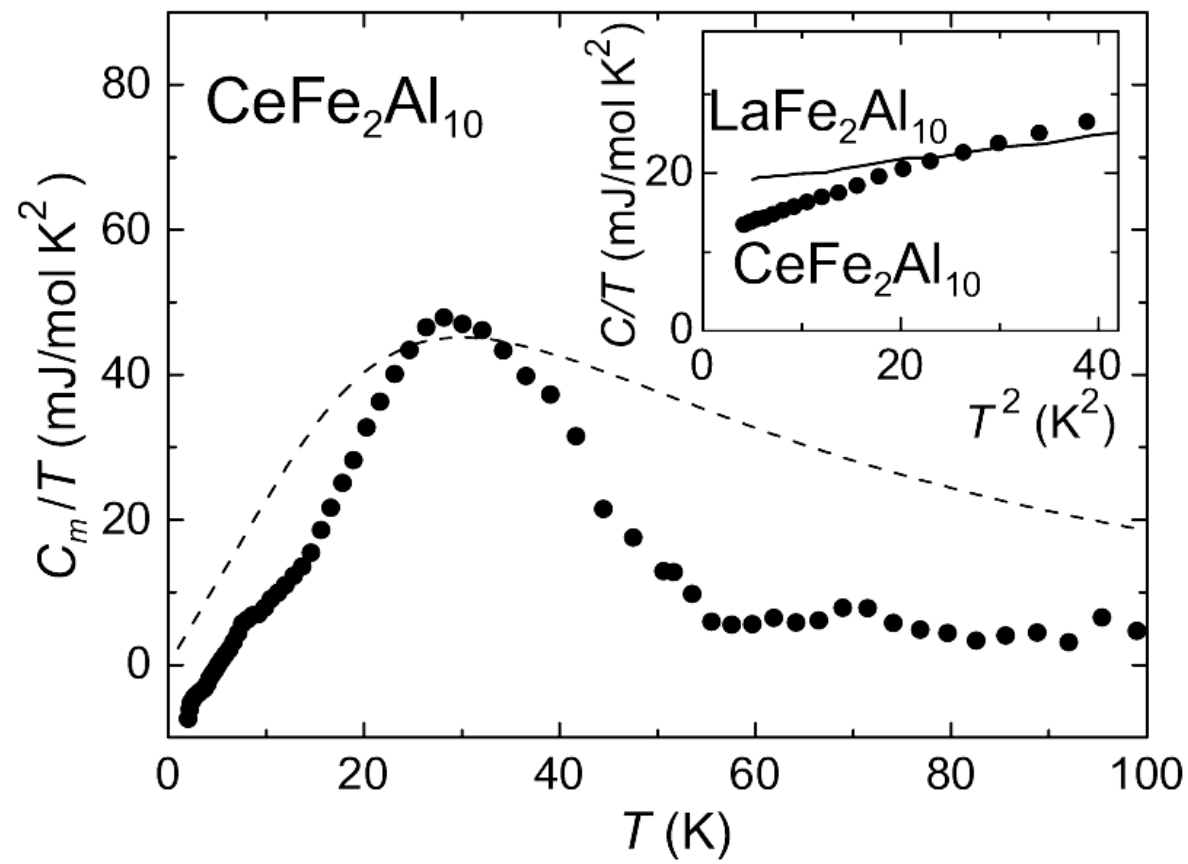


Fig. 4